SUPPLEMENTARY INFORMATION

Importance of C*–H Based Modes and Large Amplitude Motions Effects in Vibrational Circular Dichroism Spectra: The Case of the Chiral Adduct of Dimethyl Fumarate and Anthracene

Marco Passarello[1], Sergio Abbate*[1,2], Giovanna Longhi[1,2], Susan Lepri[3], Renzo Ruzziconi*[3], V. P. Nicu*[4]

[1]Dipartimento di Medicina Molecolare e Traslazionale, Università di Brescia, Viale Europa 11, 25123 Brescia, Italy

[2]CNISM Consorzio Nazionale Interuniversitario per le Scienze Fisiche della Materia,Via della Vasca Navale, 84, 00146 Roma, Italy

[3]Dipartimento di Chimica, Biologia e Biotecnologie, Università di Perugia, via Elce di Sotto 8, 06100 Italy

[4]Theoretical Chemistry, Vrjie Universiteit Amsterdam, De Boelelaan 1083, 1081 HV Amsterdam, The Netherlands

SUMMARY

SI-Section 1; Part a)

Synthesis and Characterization of adducts (*R,R*)-1, (*R,R*)-1-*d₆*, (*R,R*)-1-*d₁₆* and their respective enatiomers (*S,S*)-1, (*S,S*)-1-*d₆*, (*S,S*)-1-*d₁₆*

General. Phenanthrene, dimethyl fumarate, anhydrous aluminum trichloride, methanol-d_4 [Aldrich-Fluka (CH-9479 Buchs)], phenanthrene-d_{10} (CDN Canada) of the highest grade of purity were used without further purification. Diethyl ether was distilled from potassium hydroxide pellets in the presence of cuprous chloride, and redistilled from sodium wire in the presence of benzophenone. Dichloromethane was refluxed 5 h over phosphoric anhydride before to be distilled. Melting points were corrected after the thermometer calibration by authentic standards. ^{1}H and ^{13}C NMR spectra were recorded at 400 and 100, respectively, in CDCl$_3$ solution (if not specificated otherwise) using tetramethylsilane as the internal standard. If not specified otherwise, optical rotations were measured in solutions at 24 °C, at the sodium D-line wavelength (589 nm).

Product preparation. **Dimethyl (±)-9,10-Dihydro-9,10-ethanoanthracene-11,12-dicarboxylate [(±)-1].** Anhydrous aluminum trichloride (7.5 g, 56 mmol) and anthracene (5.0 g, 28 mmol) were added in succession, while stirring, to a solution of dimethyl fumarate (4.0 g, 28 mmol) in dry dichloromethane (100 mL) at 0 °C, under nitrogen atmosphere. The ice bath was removed and the mixture was allowed to react for 40 min at 25 °C before it was poured into ice-cold water. The organic phase was separated, the aqueous phase was extracted with dichloromethane (2 × 100 mL) and the collected organic phases were dried with sodium sulfate. After the solvent was evaporated at reduced pressure, a white solid (7.1 g, 79%) was recovered that exhibited the following characteristics: mp 107-108 °C (lit. 108–109 °C); ^{1}H NMR: δ 7.3 (m, 2H), 7.2 (m, 2H), 7.1 (m, 4H),

4.75 (s, 2H), 3.63 (s, 6H), 3.44 (m, 2H); ^{13}C NMR δ 172.8 (2C), 142.0 (2C), 140.3 (2C), 126.4 (2C), 126.3 (2C), 124.5 (2C), 123.7 (2C), 52.2 (2C), 47.8 (2C), 46.6 (2C).

(*R,R*)-(+)- and **(*S,S*)-(-)-9,10-dihydro-9,10-ethanoanthracene-11,12-dicarboxylic acid [(*R,R*)-2 and (*S,S*)-2].** Aq. sodium hydroxide (5 N, 100 mL) was added to the above crude racemic ester (7.0 g) and the mixture was kept 4 h at reflux temperature while stirring. After cooling, the mixture was extracted with diethyl ether (2 × 50 mL) and the aqueous phase was acidified at pH 4 by slow addition of 5 N aqueous hydrochloric acid (130 mL). The resulting white suspension was extracted with diethyl ether (4 × 80 mL) and the collected organic phases were dried with sodium sulfate. The solvent was evaporated at reduced pressure leaving a white solid (6.1 g, 95%) whose spectroscopic characteristic were identical to those reported in the literature for the acid (±)-**2**. The above racemic acid (6.0 g, 20 mmol) and brucine (24 g, 61 mmol) were dissolved into a mixture of azeotropic ethanol (150 mL) and water (240 mL) and heated at the reflux temperature after addition of carbon decolorizing (2.0 g). Filtration and cooling, afforded a white solid which was re-crystallized from a mixture of azeotropic ethanol (90 mL) and water (150 mL). The white solid thus obtained was treated with 5 N hydrochloric acid (50 mL), the resulting suspension was extracted with diethyl ether and the collected organic phases were dried with sodium sulfate. Solvent evaporation at reduced pressure left white prisms (2.5 g, 41 %) exhibiting the same analytical and spectroscopic properties reported in the literature for (*S,S*)-**2**: mp, 222–223 °C (lit. 219.8–220.2 °C), $[\alpha]_D^{26} = -9.9$ (c = 1.5, CH$_3$OH) [lit. $[\alpha]_D^{27} = -7.6$ (c = 1.57, CH$_3$OH)]. ^{1}H NMR (acetone-*d$_6$*) δ 10.8 (bs, 2H), 7.4 (m, 2H), 7.3 (m, 2H), 7.1 (m, 4H), 4.76 (bs, 2H), 3.41 (dd, *J* = 1.6 and 1.0 Hz, 2H).

The hydroalcoholic solution coming from the first crystallization was evaporated at reduced pressure, the remaining moist solid was treated with 5 M hydrochloric acid (100 mL) and extracted with diethyl ether (3 × 100 mL). The collected organic phase was dried with sodium sulfate, the solvent was evaporated at reduced pressure, the residual oil was crystallized from methanol and the

crystals (2.8 g, 47%) were dried at 120 °C to give a white prismatic crystals exhibiting the same characteristics reported in the literature for (*R*,*R*)-**2**: mp 224–225 °C (lit. 226–227 °C; $[\alpha]_D^{26}$ = +8.3 (c, 1.5, CH$_3$OH) [lit. $[\alpha]_D$ = +7.9 (c, 0.79, CH$_3$OH)]. ^{1}H NMR (acetone-d_6) δ 10.7 (bs, 2H), 7.4 (m, 2H), 7.3 (m, 2H), 7.1 (m, 4H), 4.77 (bs, 2H), 3.42 (dd, J = 1.7 and 1.0 Hz, 2 H).

Each of the two enantiomers (1.0 g, 3.4 mmol) was dissolved in diethyl ether (5 mL) containing a large excess of diazomethane. The mixture was made to react 2 h at 25 °C before the solvent and the excess of diazomethane was evaporated at reduced pressure. The resulting pale yellow solid was purified by chromatography on silica gel (10 g, eluent, 2 : 8 (v/v) diethyl ether-petroleum ether) to obtain the corresponding dimethyl ester.

Dimethyl (*R*,*R*)-(+)-9,10-dihydro-9,10-ethanoanthracene-11,12-dicarboxylate [(*R*,*R*)-1] (1.0 g, 95%): mp = 88-90 °C (lit. 89 - 91 °C); $[\alpha]_D^{24}$ = +29.1 (c = 1.5, CHCl$_3$) [lit. $[\alpha]_D^{27}$ = +21.19 (c 0.378, CH$_3$OH]. ^{1}H NMR δ 7.3 (m, 2H), 7.2 (m, 2H), 7.1 (m, 4H), 4.75 (s, 2H), 3.63 (s, 6H), 3.4 (m, 2H).

Dimethyl (*S*,*S*)-(–)-9,10-dihydro-9,10-ethanoanthracene-11,12-dicarboxylate [(*S*,*S*)-1] (1.1 g, 97%): mp = 88–89 °C (lit. 90 °C); $[\alpha]_D^{24}$ = −30.8 (c, 1.5, CHCl$_3$) [Lit. $[\alpha]_D^{27}$ −21.33 (c 0.1476, CH$_3$OH)]. ^{1}H NMR δ 7.3 (m, 2H), 7.2 (m, 2H), 7.1 (m, 4H), 4.74 (s, 2H), 3.63 (s, 6H), 3.43 (m, 2H).

Dimethyl (*R*,*R*)-9,10-dihydro-9,10-ethanoanthracene-11,12-dicarboxylate-d_6 [(*R*,*R*)-(+)-1-d_6] and the respective enantiomer [(*S*,*S*)-(–)-1-d_6]. Each of the above enantiomeric acids (*R*,*R*)-**2** or (*S*,*S*)-**2** was converted into the corresponding methyl ester-d_6 as follows. A mixture of the acid (1.0 g, 3.4 mmol) and thionyl chloride (5.0 mL, 8.2 g, 69 mmol) in toluene (25 mL) was heated at the reflux temperature until the solid was completely dissolved (3.5 h). The solvent and the excess of thionyl chloride were evaporated at reduced pressure, the residual oil was dissolved in methanol-

d_4 (20 mL), and the mixture was refluxed for 2 h in the presence of pyridine (1 mL). After the solvent evaporation, the residue was dissolved into diethyl ether (25 mL) and washed first with 0.5 M aqueous sulfuric acid (25 mL), then with saturated aqueous sodium hydrogencarbonate (25 mL) and finally with water (25 mL). The organic phase was dried with sodium sulfate and the solvent was evaporated at reduced pressure. Chromatography of the residual oil on silica gel (30 g, eluent, 2:8 (v/v) diethyl ether-petroleum ether) allowed to collect the pure dimethyl ester (0.8 g, 73%) exhibiting the following characteristics.

(R,R)-(+)-1-d_6 (0.81 g, 73%): mp 89–90°C; $[\alpha]_D^{24}$ = +7.0 (c, 1.5 CH$_3$OH); ^{1}H NMR: δ 7.3 (m, 2H), 7.2 (m, 2H), 7.1 (m, 4H), 4.72 (s, 2H), 3.42 (m, 2H);

(S,S)-(–)-1-d_6 (0.84 g, 75%): mp 88–90 °C; $[\alpha]_D^{20}$ = -7.8 (c, 1.5 CH$_3$OH). ^{1}H NMR: δ 7.3 (m, 2H), 7.2 (m, 2H), 7.1 (m, 4H), 4.78 (s, 2H), 3.49(m, 2H);

Dimethyl (R,R)-(+)- 9,10-dihydro-9,10-ethanoanthracene-11,12-dicarboxylate-d_{16} [(R,R)-1-d_{16}] and the respective enantiomer[(S,S)-1-d_{16}] were prepared analogously from anthracene-d_{10} (5.0 g, 27 mmol) and dimethyl fumarate (4.0 g, 28 mmol). Racemic **Dimethyl (±)-9,10-dihydro-9,10-ethanoanthracene-11,12-dicarboxylate-d_{10} [(±)-1-d_{10}]** (6.7 g, 76%) was obtained exhibiting the following characteristics: mp 108–109 °C; ^{1}H NMR δ 3.63 (s, 6H), 3.41 (s, 2H).

As for **(±)-2**, after alkaline hydrolysis of the ester **(±)-1-d_{10}** (6.0 g, 18 mmol) gave the racemic acid [**(±)-9,10-dihydro-9,10-ethanoanthracene-11,12-dicarboxylic acid-d_{10} [(±)-2-d_{10}]** (5.4 g, 98%) [mp 250–251 °C. ^{1}H NMR (acetone-d_6) δ 10.45 (bs, 2H), 3.41 (s, 2H)] which was resolved into the enantiomers (R,R)-2-d_{10} and (S,S)-2-d_{10} by fractional crystallization of their diastereomeric brucine salts.

Both the enantiomeric acid (*R,R*)-**2**-d_{10} and (*S,S*)-**2**-d_{10} were treated with thionyl chloride as described above for the preparation of (*R,R*)-**1**-d_6 and (*S,S*)-**1**-d_6 and the resulting acyl chlorides were refluxed 2 h in methanol-d_4. The usual work-up gave the following products as white prisms exhibiting the following characteristics.

(*R,R*)-**1**-d_{16}: mp, 91-92 °C; $[\alpha]_D^{24}$ = +18 (c = 1.5, CH$_3$OH); ^{1}H NMR δ 3.41 (s, 2H); ^{13}C NMR δ 172.7 (2C), 141.8 (2C), 140.1 (2C), 125.8 (t, *J* = 24 Hz, 2C), 125.7 (t, *J* = 24 Hz, 2C), 124.0 (t, *J* = 24 Hz, 2C), 123.2 (t, *J* = 24 Hz, 2C), 51.4 (sept, *J* = 22 Hz, 2C), 47.6 (2C) 46.1 (t, *J* = 21 Hz, 2C).

(*S,S*)-**1**-d_{16}: mp = 88-89 °C; $[\alpha]_D^{24}$ = –20 (c = 1.5, CH$_3$OH). ^{1}H NMR δ 3.40 (s, 2H); ^{13}C NMR δ 172.6 (2C), 141.8 (2C), 140.0 (2C), 125.7 (t, *J* = 24 Hz, 2C), 125.7 (t, *J* = 24 Hz, 2C), 124.1 (t, *J* = 24 Hz, 2C), 123.1 (t, *J* = 24 Hz, 2C), 51.4 (sept, *J* = 22 Hz, 2C), 47.5, 46.1 (t, *J* = 21 Hz, 2C).

Useful References

[20] M.-J. Brienne, J. Jacques *Bull. Soc. Chim. Fr.* **1973**, *1*, 190–197.

[21] L. Thunberg, S. Allenmark *Tetrahedron: Asymmetry* **2003**, *14*, 1317–1322.

[22] C. R. Ramanathan, M. Periasamy *Tetrahedron: Asymmetry* **1998**, *9*, 2651–2656.

[23] Hagishita, S.; Kuriyama, K. *Tetrahedron*, **1972**, *28*, 1435-1467.

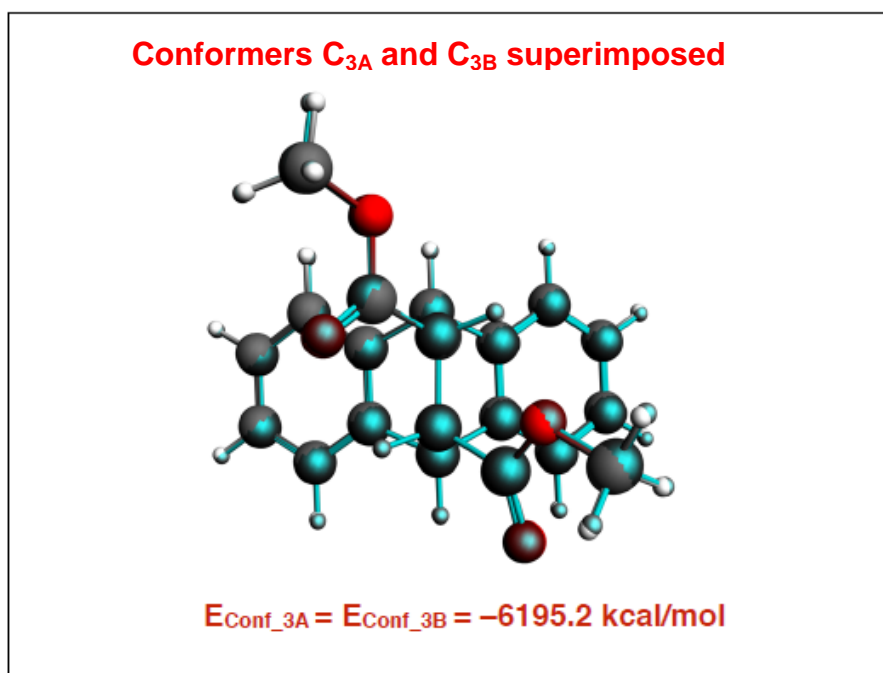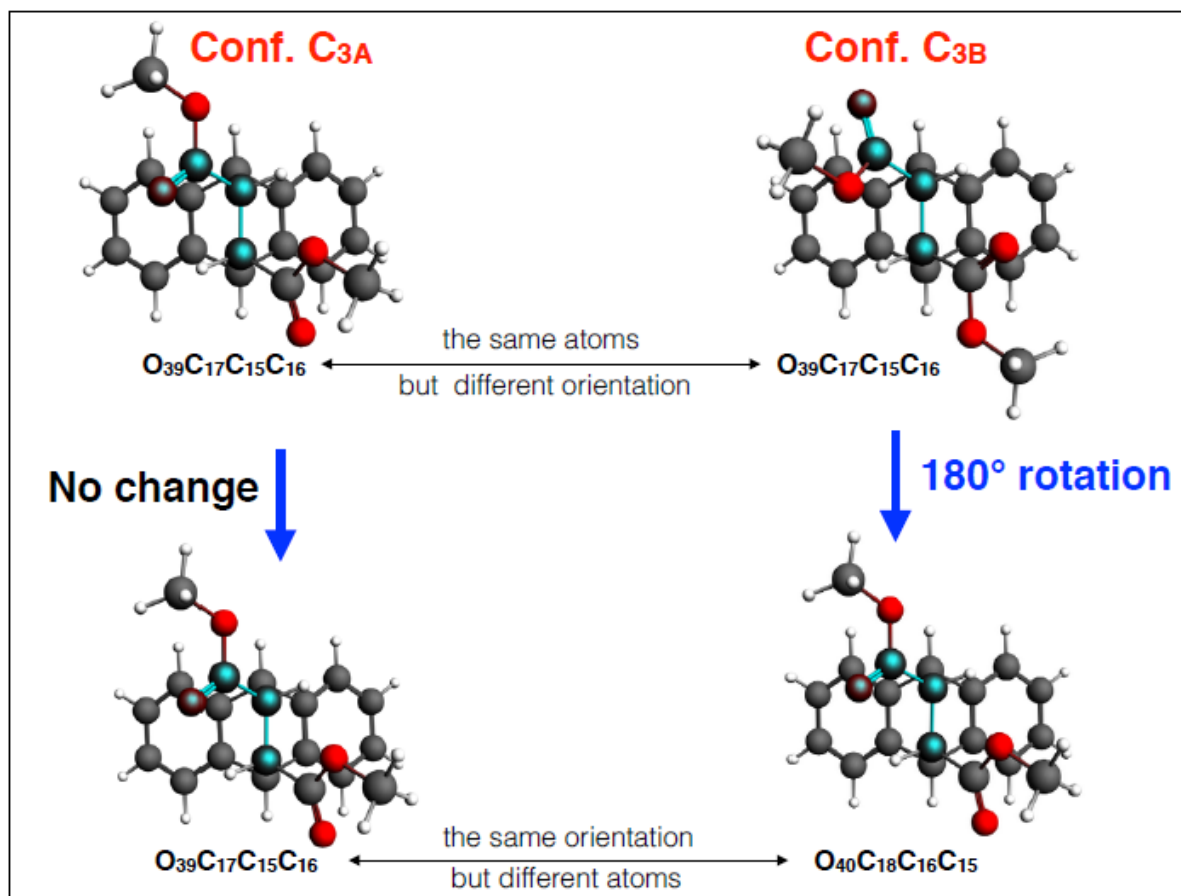[24] M.-J. Brienne, J. Jacques *C. R. Acad. Sc. C* **1971**, *272*, 1889–1891.

SI-Section 1 ; Part b)

ECD and UV spectra of dimethyl (*S*,*S*)-(-)-9,10-dihydro-9,10-ethanoanthracene-11,12-

dicarboxylate and its enantiomer dimethyl (*R*,*R*)-(-)-9,10-dihydro-9,10-ethanoanthracene-11,12-

dicarboxylate in CH_3CN solution.
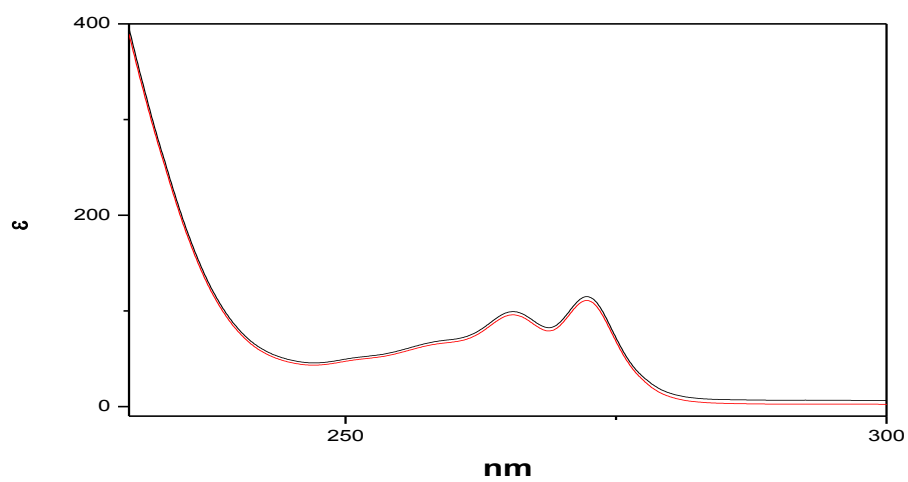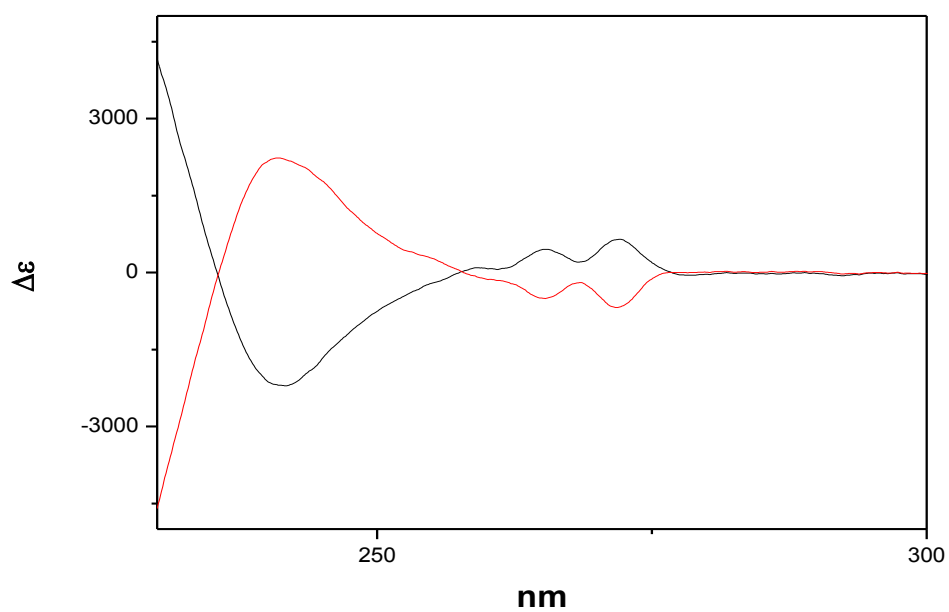
SI- Section 2: Conformers C^3_A and C^3_B

Figure 1: The two realisations of conformer C^3.

Conf. C$_{3A}$

Conf. C$_{3B}$

O$_{39}$C$_{17}$C$_{15}$C$_{16}$ ←——→ O$_{39}$C$_{17}$C$_{15}$C$_{16}$

the same atoms
but different orientation

No change

180° rotation

O$_{39}$C$_{17}$C$_{15}$C$_{16}$ ←——→ O$_{40}$C$_{18}$C$_{16}$C$_{15}$

the same orientation
but different atoms

Conformers C$_{3A}$ and C$_{3B}$ superimposed

$E_{Conf\_3A} = E_{Conf\_3B} = -6195.2$ kcal/mol

SI- Section 3: Values of the Anthracene Angle for the Conformers investigated in the LT Study

Variation of the anthracene dihedral angle during the LT scan in $C^2 - (DCCl_3)_2$

LT parameter	Anthracene
5.9	122.8
2.9	122.9
359.9	122.9
356.9	123.0
353.9	123.0
350.9	123.1
347.9	123.2
344.9	123.3
341.9	123.3
338.9	123.5
335.9	123.5
332.9	123.6
329.9	123.7
326.9	123.8
323.9	123.9
320.9	123.9
317.9	124.0
5.9	122.8
8.9	122.8
11.9	122.8
14.9	122.7
17.9	122.6
20.9	122.5
23.9	122.4
26.9	122.4
29.9	122.3
32.9	122.3
35.9	122.1
38.9	122.1
41.9	122.1
44.9	122.0
47.9	122.0
50.9	121.9
53.9	122.0

Variation of the anthracene dihedral angle during the LT scan in $C^3 - (DCCl_3)_2$

LT parameter 1	LT parameter 2	Anthrachene
2.7	202.9	123.3
352.7	205.5	123.4
342.7	206.3	123.6
332.7	208.2	123.7
322.7	210.4	123.9
312.7	211.0	123.9
302.7	209.6	123.9
2.7	202.9	123.3
12.7	201.3	123.2
22.7	197.6	123.2
32.7	194.9	123.1
42.7	190.9	123.1
52.7	186.8	123.1
62.7	183.5	123.1

SI section 4: Vacuum, COSMO and LT calculations for C^2 and $C^3 - (DCCl_3)_2$
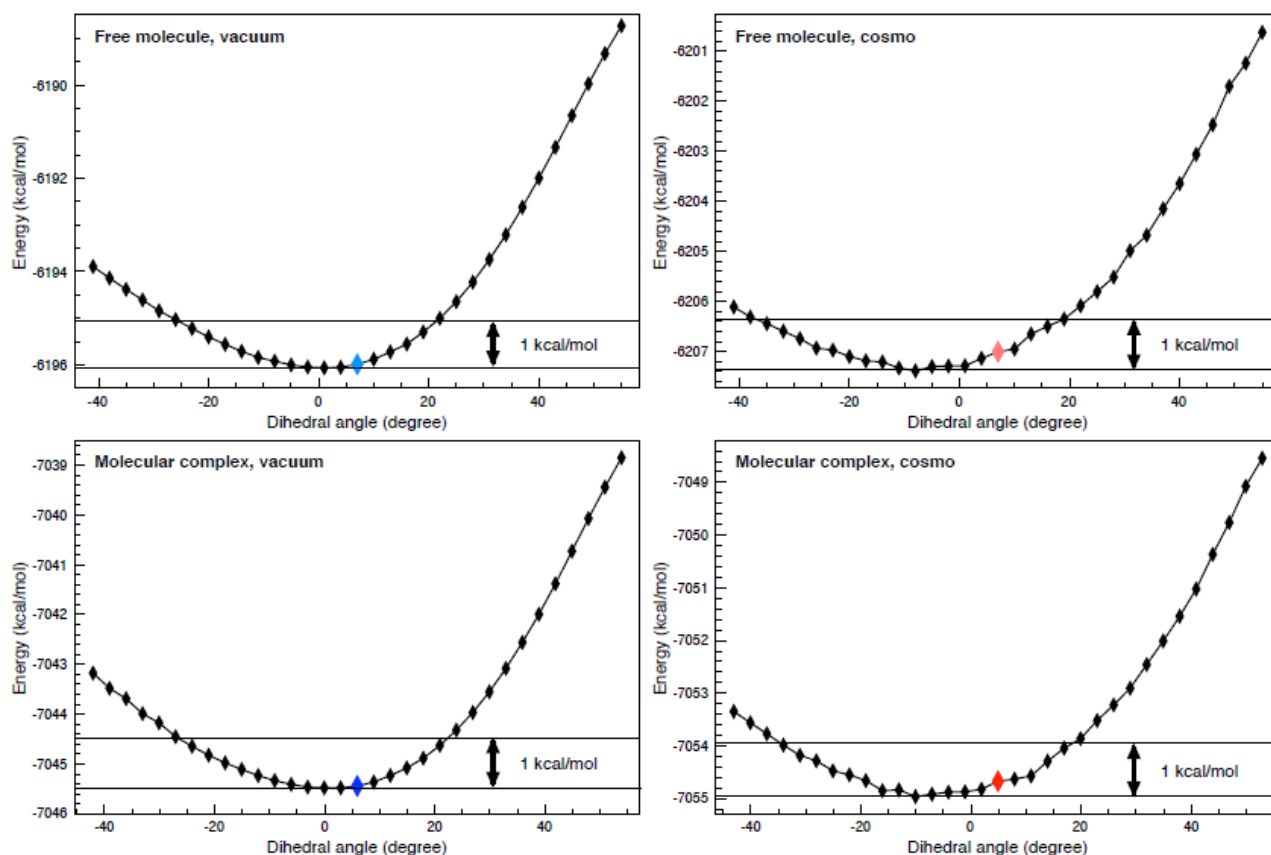
Figure 2: Dependence of the total bonding energy (TBE) on the LT parameters. The colored symbol in each energy plot indicates the starting point in the LT calculations, i.e. the energy of the reference structure.
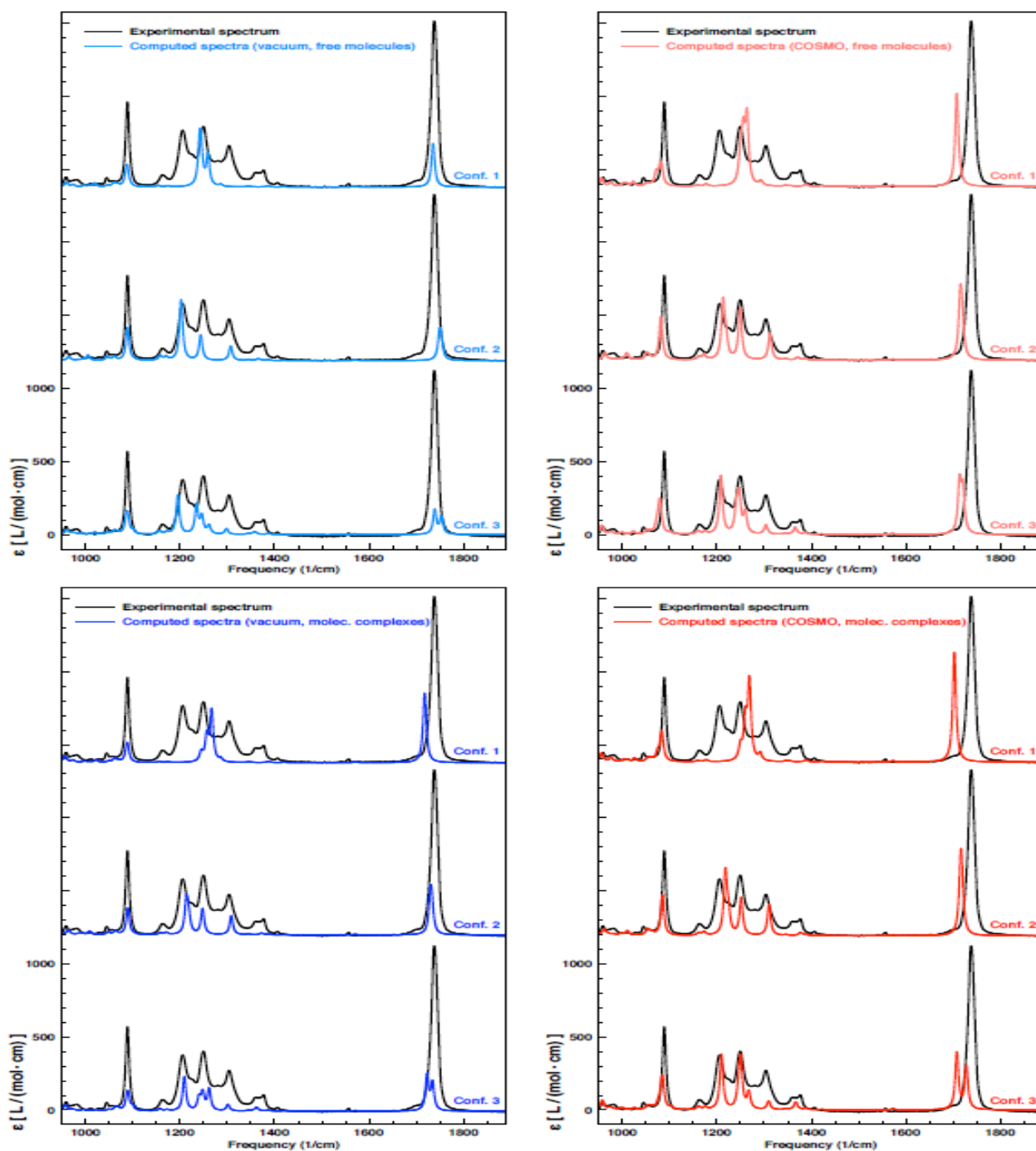
Figure 3: Vibrational absorption spectra in the fingerprint region. Comparison between the experimental spectrum (black) and the spectra computed for the three conformers (colored). Four types of calculations have been performed: a) vacuum calculations for the free conformers (upper left), b) COSMO calculations for the free conformers (upper right), c) vacuum calculations for the molecular complex formed by one conformer and two $DCCl_3$ solvent molecules (lower left), d) COSMO calculations for the molecular complex formed by one conformer and two $DCCl_3$ solvent molecules (lower right)
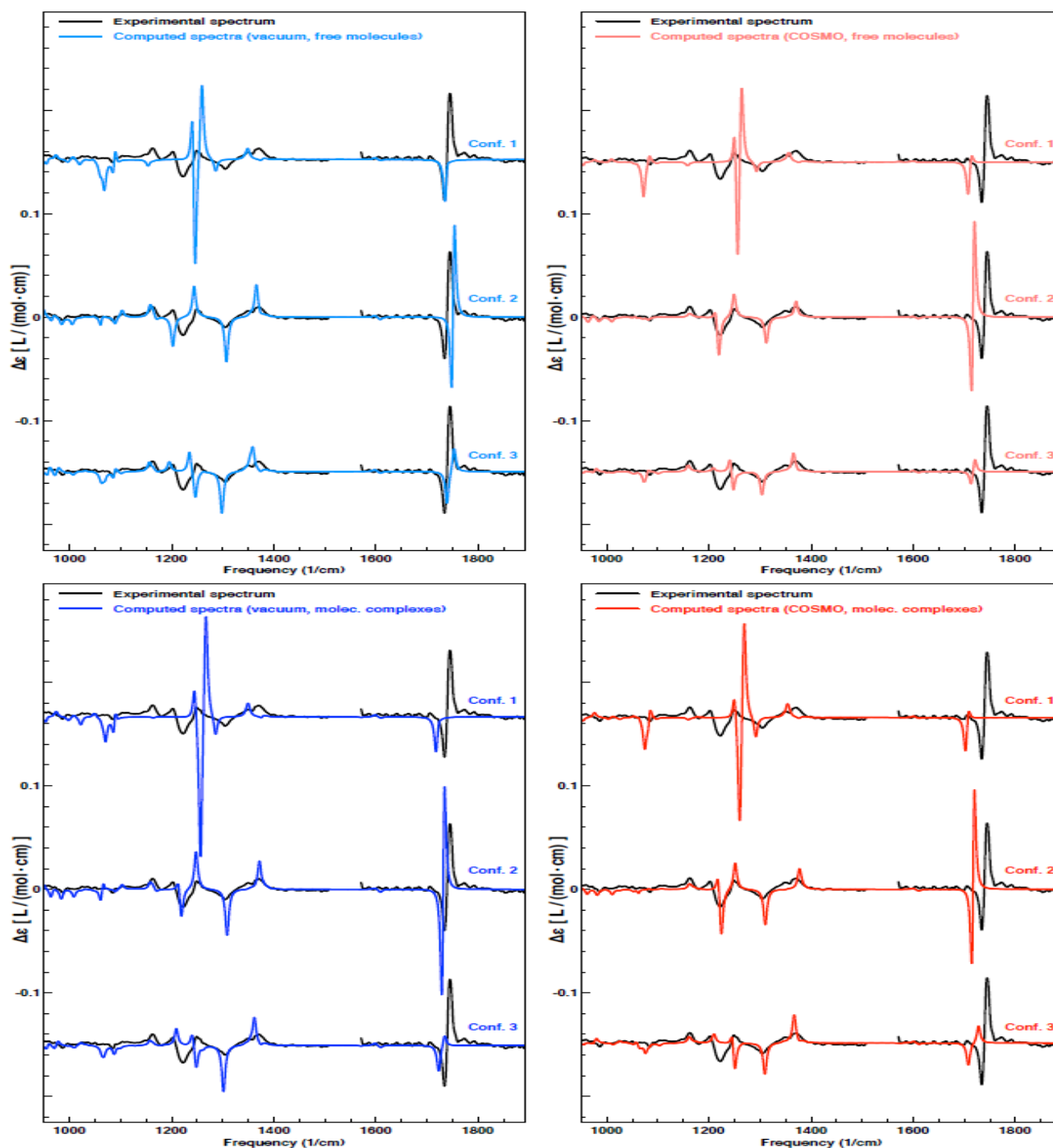
Figure 4: Vibrational circular dichroism spectra in the fingerprint region. Comparison between the experimental spectrum (black) and the spectra computed for the three conformers (colored). Four types of calculations have been performed: a) vacuum calculations for the free conformers (upper left), b) COSMO calculations for the free conformers (upper right), c) vacuum calculations for the molecular complex formed by one conformer and two DCCl$_3$ solvent molecules (lower left), d) COSMO calculations for the molecular complex formed by one conformer and two DCCl$_3$ solvent molecules (lower right)
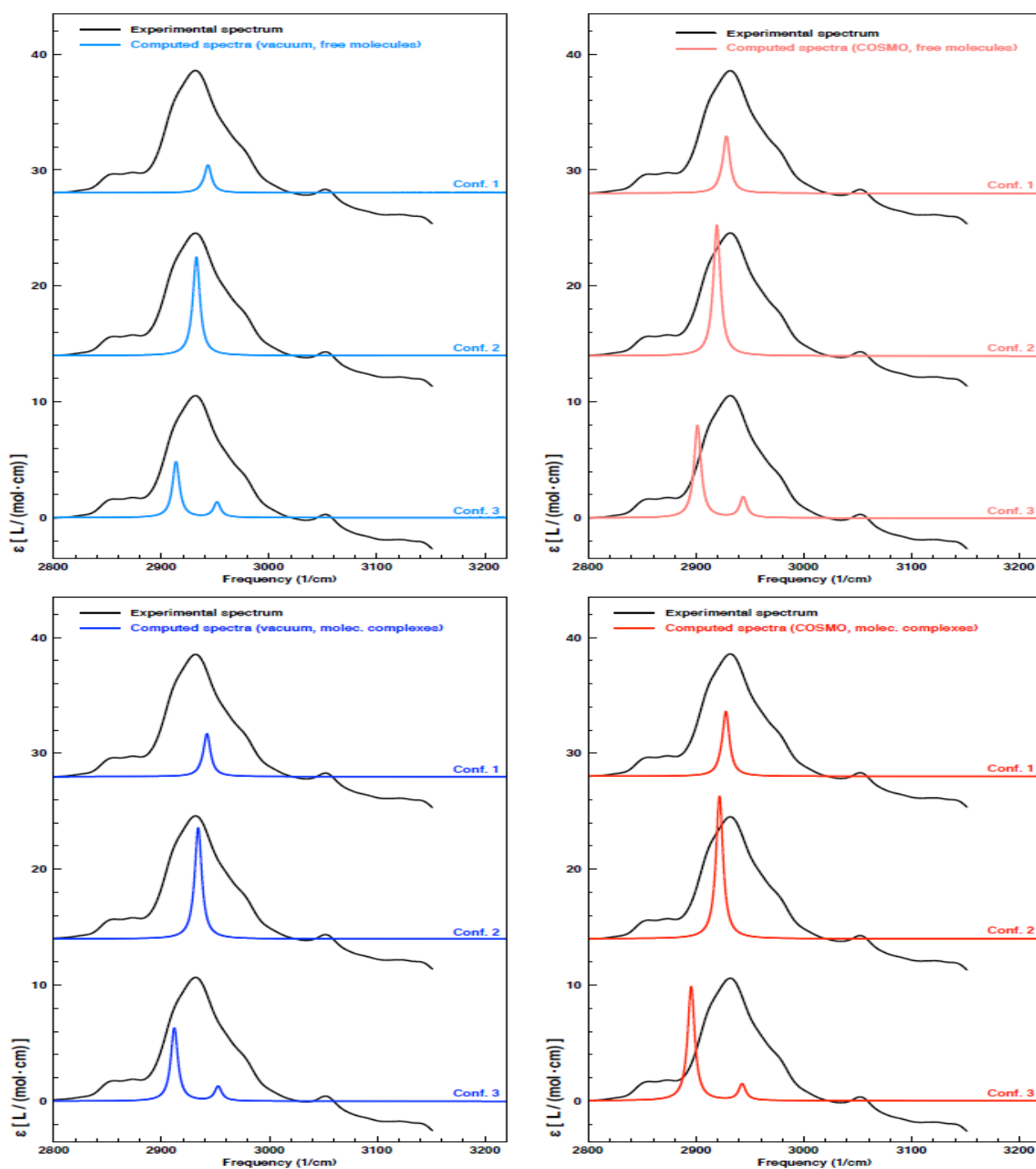
Figure 5: Vibrational absorption spectra in the CH-stretching region. Comparison between the experimental spectrum (black) and the spectra computed for the three conformers (colored). Four types of calculations have been performed: a) vacuum calculations for the free conformers (upper left), b) COSMO calculations for the free conformers (upper right), c) vacuum calculations for the molecular complex formed by one conformer and two $DCCl_3$ solvent molecules (lower left), d) COSMO calculations for the molecular complex formed by one conformer and two $DCCl_3$ solvent molecules (lower right)
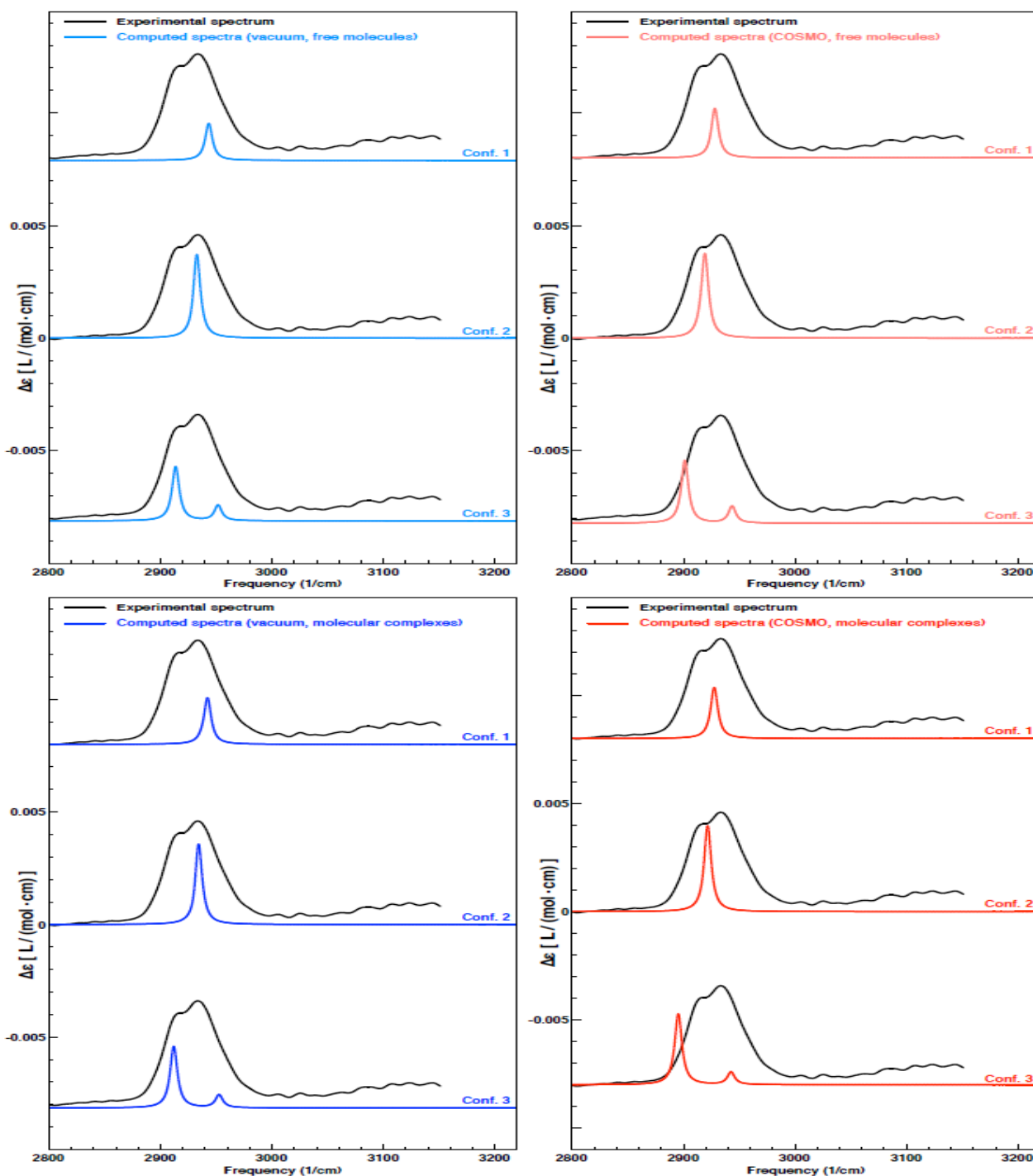
Figure 6: Vibrational circular dichroism spectra in the CH-stretching region. Comparison between the experimental spectrum (black) and the spectra computed for the three conformers (colored). Four types of calculations have been performed: a) vacuum calculations for the free conformers (upper left), b) COSMO calculations for the free conformers (upper right), c) vacuum calculations for the molecular complex formed by one conformer and two $DCCl_3$ solvent molecules (lower left), d) COSMO calculations for the molecular complex formed by one conformer and two $DCCl_3$ solvent molecules (lower right)
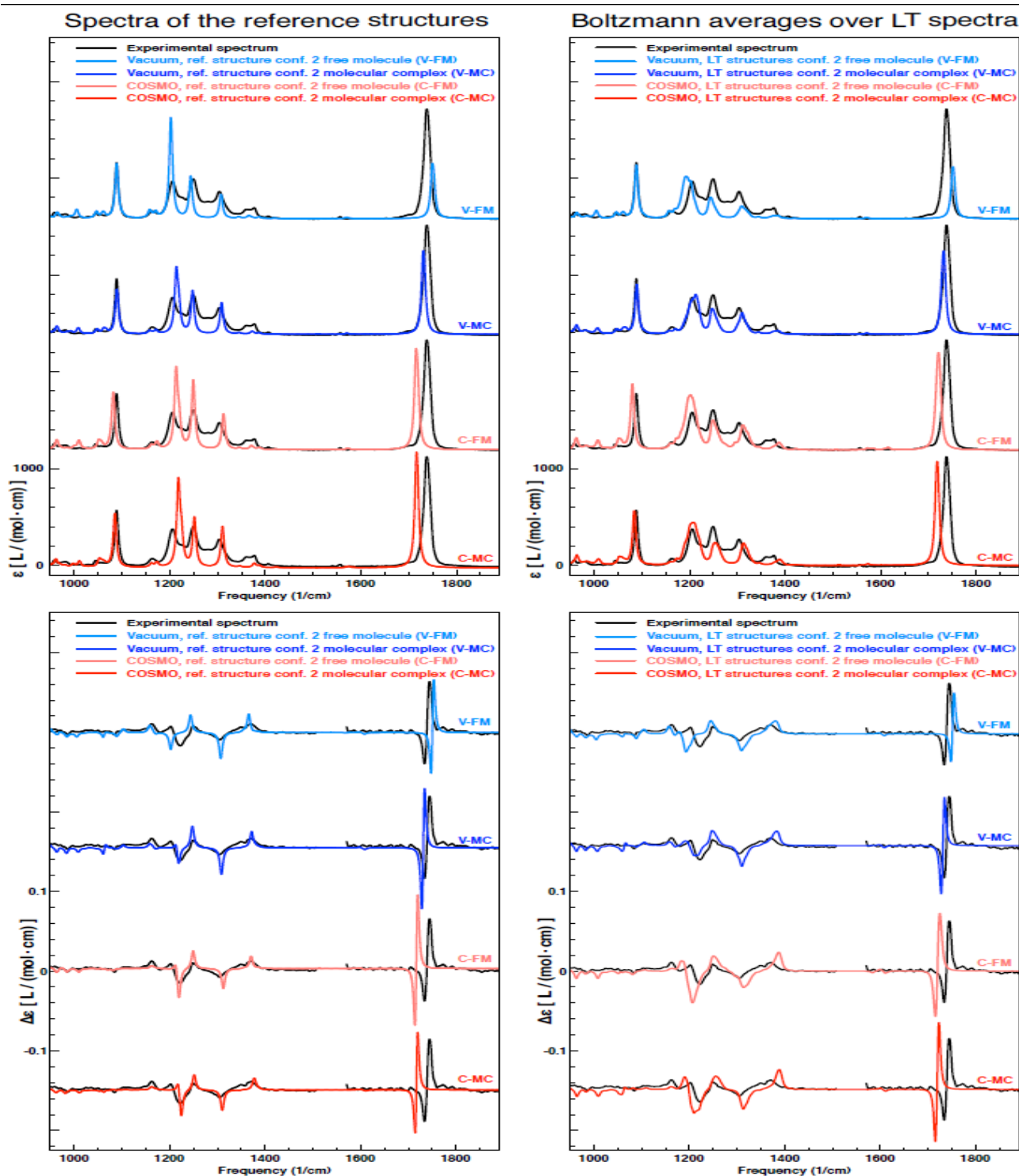
Figure 7: Fingerprint region. Comparison between the experimental VA and VCD spectra (black) and 1) the spectra computed for conformer C^2 (plots on the left), and 2) the Boltzmann weighted spectra obtained by averaging over all linear transit structures obtained for conformer C^2 (plots on the right). Four types of calculations have been performed: a) vacuum calculations for the free conformers (V-FM), b) COSMO calculations for the free conformers (C-FM), c) vacuum calculations for the molecular complex formed by one conformer and two $DCCl_3$ solvent molecules (V-MC), d) COSMO calculations for the molecular complex formed by one conformer and two $DCCl_3$ solvent molecules (C-MC).
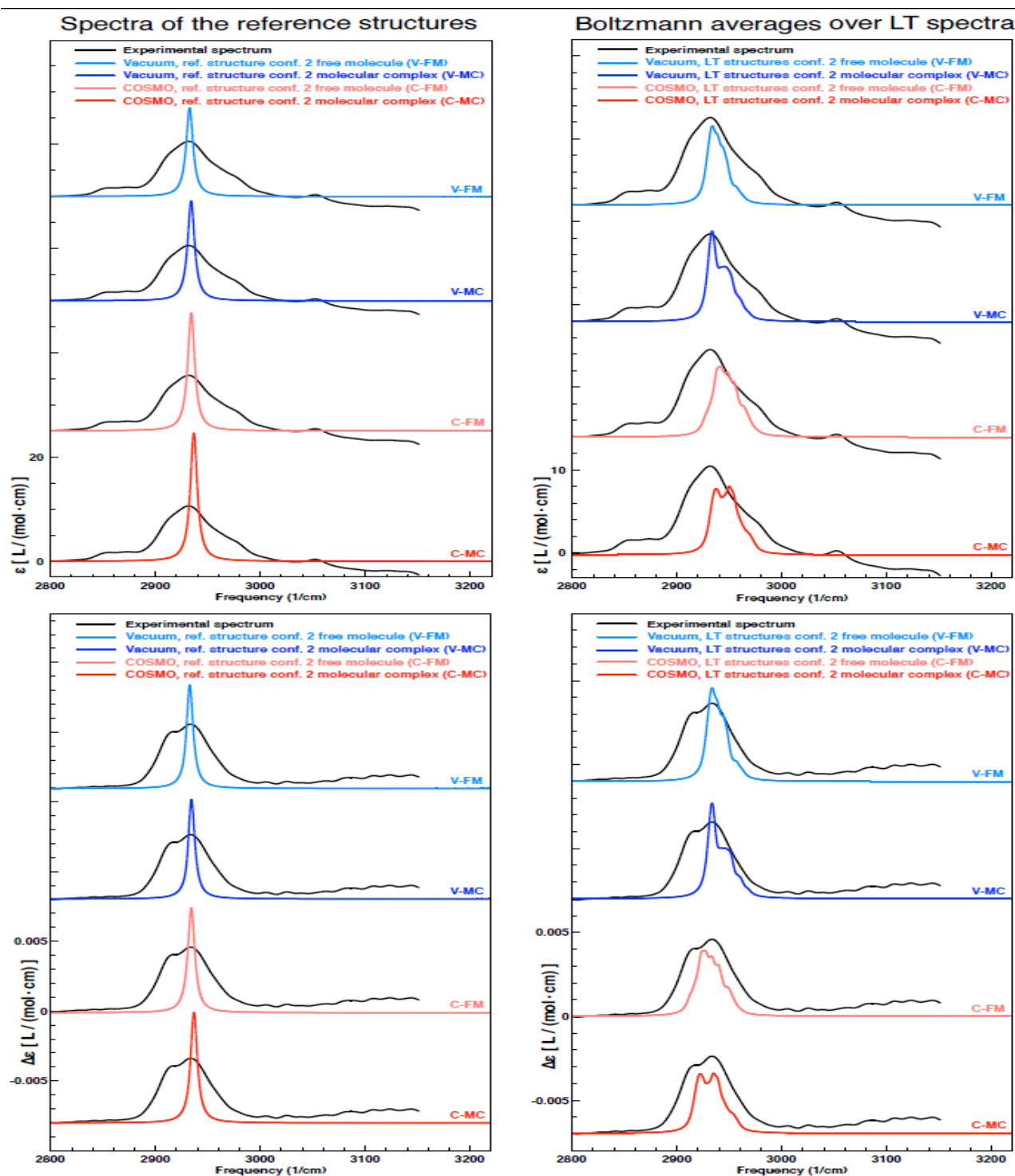
Figure 8: CH-stretching region. Comparison between the experimental VA and VCD spectra (black) and 1) the spectra computed for conformer C^2 (plots on the left), and 2) the Boltzmann weighted spectra obtained by averaging over all linear transit structures obtained for conformer C^2 (plots on the right). Four types of calculations have been performed: a) vacuum calculations for the free conformers (V-FM), b) COSMO calculations for the free conformers (C-FM), c) vacuum calculations for the molecular complex formed by one conformer and two DCCl$_3$ solvent molecules (V-MC), d) COSMO calculations for the molecular complex formed by one conformer and two DCCl$_3$ solvent molecules (C-MC).

SI- Section 5: Comparison of Calculated VA and VCD spectra in the fingerprint and CH-stretching region for (R,R)-1 and (R,R)-1-d_{16} for conformer C^2
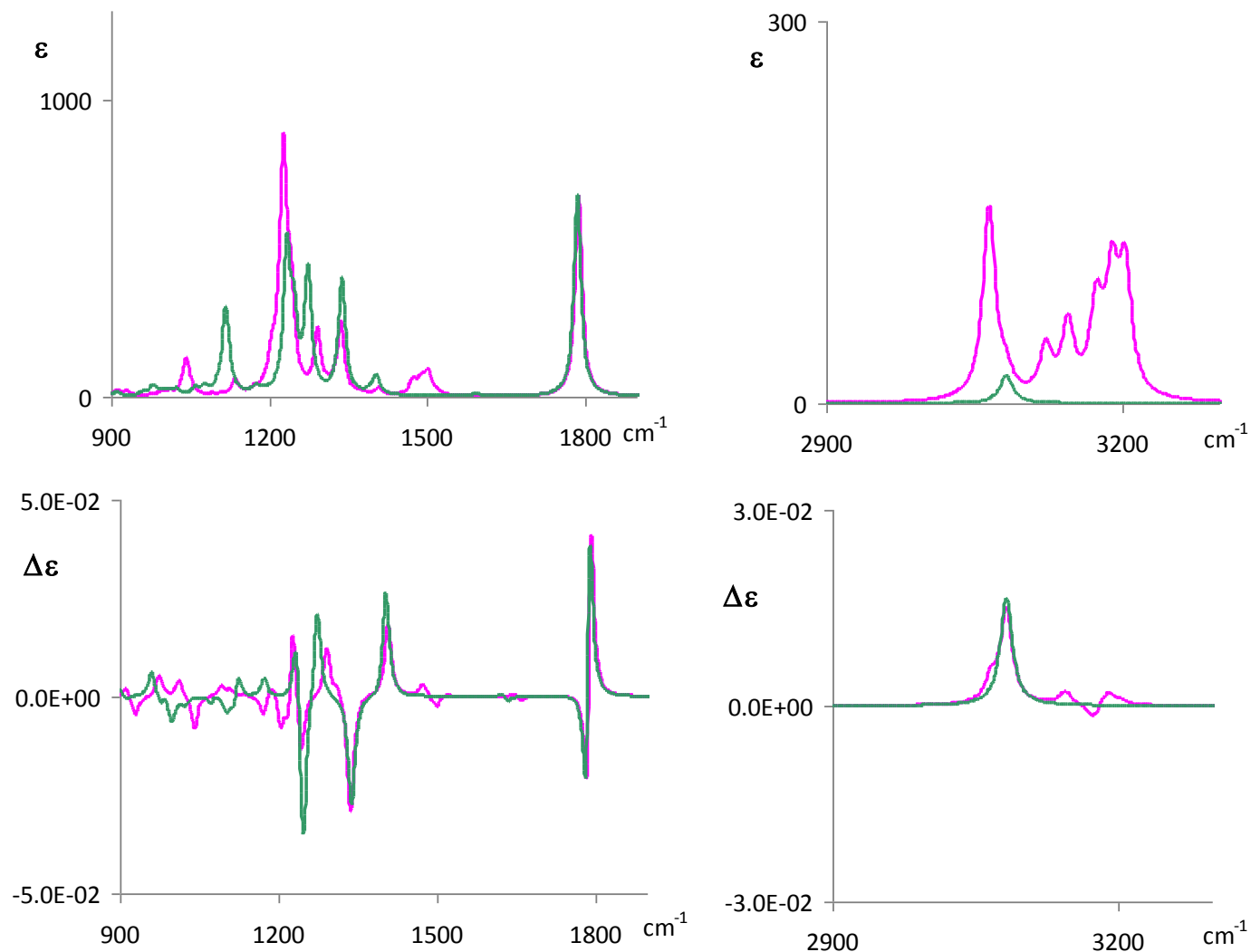
Superposition of calculated VA and VCD spectra of (R,R)-**1** (pink) and (R,R)-**1**-d_{16} (green) for the case of the dominant conformer C^2 (vacuum case). VCD spectra in the CH stretching region consist of just one feature irrespective of the compound considered (undeuterated, d_6 or d_{16}) as shown in Figure 1 in the text. This is well accounted for also by calculations, as can be seen from the above plots.